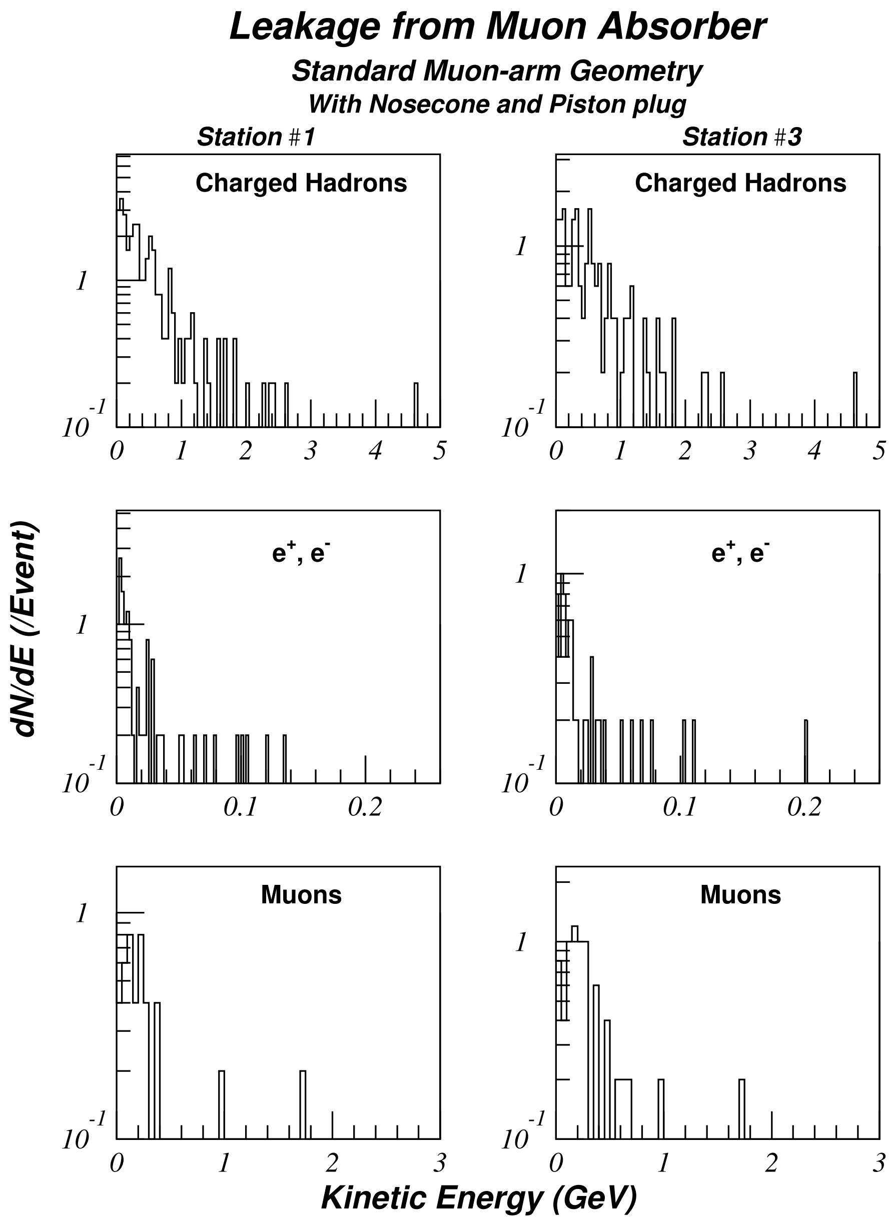

Figure 10.26: Kinetic energy spectra of charged hadrons, electrons and positrons, and muons reaching muon tracking stations #1 and #3 as obtained from GEANT simulations for the standard muon absorber geometry with Cu piston plug and Cu nosecone. The bin sizes are 50 MeV for hadrons and muons and 2 MeV for electrons and positrons.

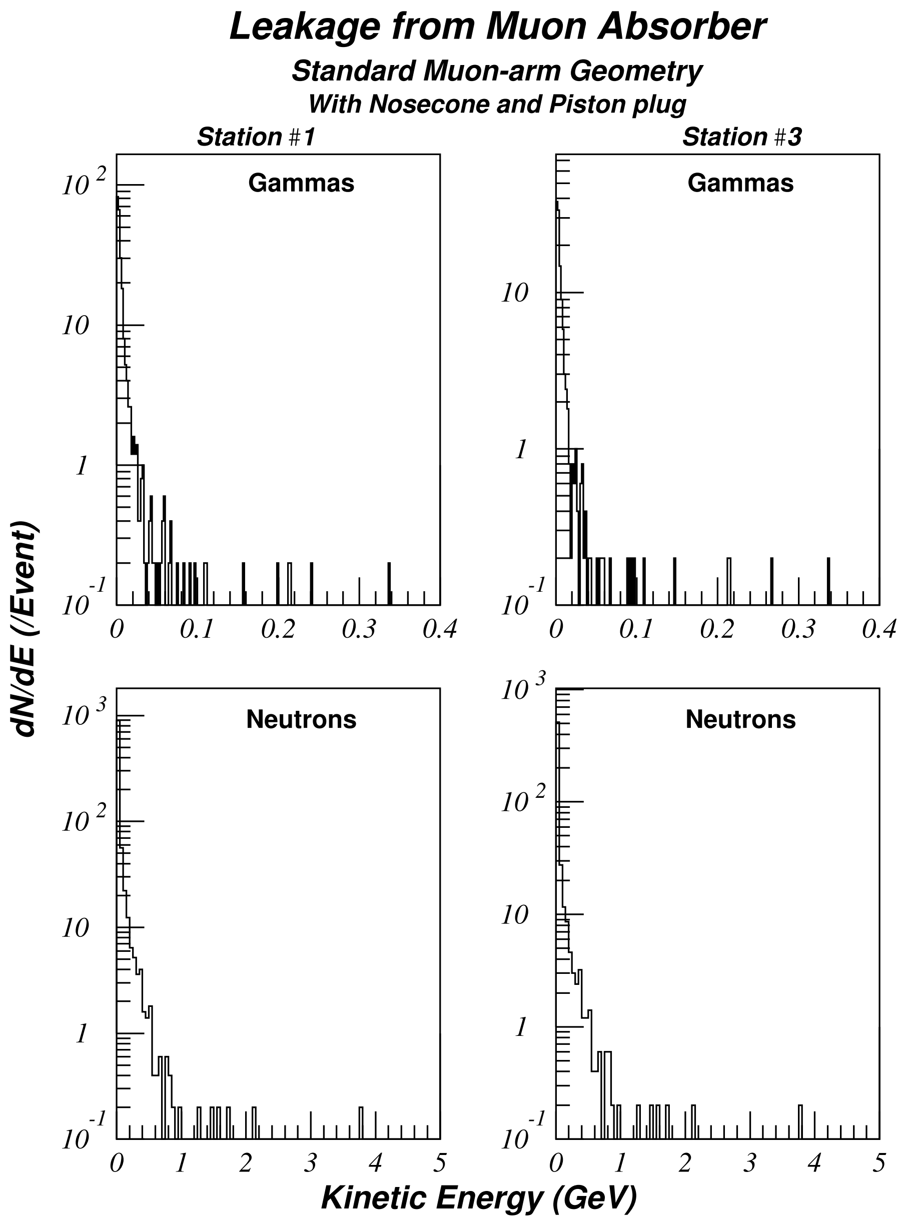

Figure 10.27: Kinetic energy spectra of photons and neutrons reaching muon tracking stations #1 and #3 as obtained from GEANT simulations for the standard muon absorber geometry with Cu piston plug and Cu nosecone. The bin sizes are 50 MeV for neutrons and 2 MeV for photons.

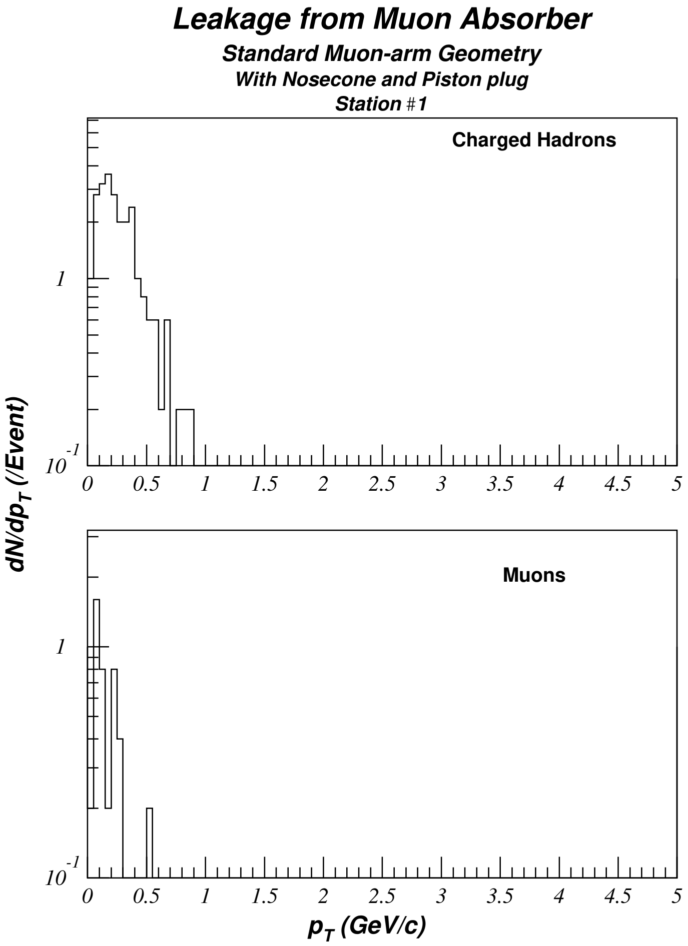

Figure 10.28: Transverse momentum (p_T) spectra of charged hadrons and $\mu^{\pm}$ reaching muon tracking station #1. The bin size is 50 MeV/c.

probability of decay muons having energies greater than 1 GeV. Fig.10.26 shows that there is also a sizeable number of charged hadrons with energies greater than 1 GeV. Most of these charged hadrons are below 3.0 GeV and can be distinguished from muons by the muon identifier. The mean p_T of the decay muons as well as of the charged hadrons is quite small ($<$ 1 GeV/c for charged hadrons and $<$ 0.5 GeV/c for $\mu^{\pm}$) as can be seen from Fig. 10.28, which helps in rejection.

There are orders of magnitude more low energy ($<$ 100 MeV) neutrons than charged hadrons. The neutrons, however, should not present a crippling problem for the muon spectrometer because of the expected very small chamber efficiency for neutrons. However, R&D work to quantify the tracking chamber response to neutrons is necessary. Most of the photon flux is below 25 MeV. Although pair production in the chambers from these photons is a concern, it can be minimized by putting as little material in their way as possible. This is also necessary to obtain the best momentum resolution from the chambers, as noted below in Fig. 10.30.

The Level of particle leakage into the muon arm is an important issue for the PHENIX trigger. The muon arm trigger constructs a list of candidate tracks with one hit each in stations #2 and #3, compares this to deep hits in the muon identifier, and then to hits in station #1 corresponding to allowed trajectories. The initial list of candidates used to mask the tracking chamber lists is derived from hits deep in the muon identifier. Charged particles leaving the event vertex with less than 2 GeV kinetic energy, or less than about 1 GeV kinetic energy after the lead shield behind the central magnet pole tip, do not penetrate deeply enough into the muon identifier to satisfy this LVL-1 trigger. This fact was used as a guide in determining when the hadron absorber was thick enough to result in an acceptably small false trigger rate. The leakage rates also determine how many combinatorial pairs (which dominate the real pair rate) the LVL-2 trigger must process through the above algorithm, and the resulting total time required for the muon LVL-2 trigger.

10.4.2 Tracking and Spectrometer

Track Reconstruction Algorithm

Three different algorithms, all of which give essentially equivalent results, were used to reconstruct the muon momentum at the vertex from the hit positions in the three tracking stations and the vertex position. The first algorithm, developed at Vanderbilt, was based on visually inspecting the PISA output for the correlation between the original momentum and the hit positions in polar coordinates. The second was based on the algorithms developed for the experiments E772/789 at Fermilab. The third algorithm was developed at ORNL and uses an expansion of the original vertex momentum in terms of Legendre polynomials with the variables consisting of appropriately scaled hit positions in polar coordinates. The expansion coefficients were determined to arbitrarily large order by chi-squared minimization. This method is particularly well suited for use in a LVL-2 trigger, since it requires only a few hundred simple multiplications and additions.

The tracking procedure for the spectrometer consists of two steps: (1) finding the track segments from the hits in each station, and (2) joining the track segments from the three stations.

The track reconstruction uses simple tree searches for correlated hit candidates combined with a Principal Component Analysis (PCA) test [6] to select the correct candidates. Let us assume a single track generates a M-dimensional hit vector $\vec{h} = (h_1, h_2, .., h_i, .., h_M)$. For step (1) the hits are the hit positions in each of the six drift chambers in the $UU'YY'VV'$ geometry. For step (2) the first four coordinates in the hit vector (h_1, h_2, h_3, h_4) will be the θ and ϕ of the track segment position and the θ and ϕ of the track segment local direction vector within the first tracking station. The next four coordinates will be the same track segment information from the second tracking station.

The algorithm is tuned using "learning tracks"; from PISA simulations N learning tracks $\vec{h}_n$ are generated ($N > 1000$) and the following average hit vector $\vec{H}$ and dispersion matrix

A are created

$$H_i = \frac{1}{N}\sum_{n=1}^{N}(h_i)_n$$
$$A_{ij} = \frac{1}{N}\sum_{n=1}^{N}[(h_i)_n - H_i][(h_j)_n - H_j]$$

It is important to note that at a more advanced stage of the experiment the N learning tracks should not be taken from simulations, but instead from low multiplicity calibration data.

Finally the M eigenvalues λ_i and M eigenvectors $\vec{\omega}_i$ of the dispersion matrix **A** are calculated. The eigenvalues can be organized as a vector $\vec{\lambda}$ and the eigenvectors can be organized into a $M \times M$ matrix ω with components ω_{ij}.

Based on $\vec{\lambda}$ and ω it is now possible to use the following very sensitive criteria to test if a track candidate $\vec{c} = (c_1, c_2, .., c_i, .., c_M)$ constitutes a true track. The generalized distance, d, of $\vec{c}$ from an ideal track can be defined as

$$\eta_j = \sum_{i=1}^{M}\omega_{ij}(c_i - H_i)$$
$$d^2 = \frac{1}{M}\sum_{j=1}^{M}\frac{\eta_j^2}{\lambda_j}$$

d will be approximately normally distributed with a standard deviation of 1. If d is *not* normally distributed then the learning data set contains abnormalities and should be carefully analyzed. If it is now required for a track candidate that $d < d_{\max}$, then only a small fraction of all real tracks will be rejected, whereas a very large fraction of spurious tracks will be rejected. For $d_{\max} = 3$ only 0.3% of the real tracks are rejected. The fraction rejected depends on the relative magnitude of the eigenvalues. In a high resolution detector, the smallest eigenvalues become extremely small and the rejection power of the PCA test is very good. The PCA test constitutes the best possible rejection test based on a linear method; the linearity ensures that the PCA is a very fast rejection test.

The track segment finding within a tracking station proceeds according to the following scheme:

1. First, all possible UU', YY' and VV' hit pairs are identified by searchin for hit positions in the two planes smaller than $L_p\times$ the plane separation. where L_P is typically 2–3. The average position $\overline{h}_k$ for each of the possible pairs is calculated.

2. A PCA test with $d_{\max} = 5$ is applied to all sets of 3 pairs, (UU', YY' and VV'. Due to the large value of $d_{\max}$ this first test keeps all real tracks, but rejects the obviously false cases and reduces the total number of track candidates substantially.

3. A more sensitive PCA test with $d_{\max} = 4$ is now applied to the complete 6-dimensional set of possible hits surviving step 2.